pH, Electrolyte, and Substrate-Linked Variation in Active Site Structure of the Trp51Ala Variant of Cytochrome *c* Peroxidase†

Paola Turano,‡ Juan C. Ferrer,§,|| Myles R. Cheesman,⊥ Andrew J. Thomson,⊥ Lucia Banci,‡ Ivano Bertini,*,‡ and A. Grant Mauk*,§

Department of Chemistry, University of Florence, Florence, Italy, Department of Biochemistry and Molecular Biology, University of British Columbia, Vancouver, V6T 1Z3 Canada, and School of Chemical Sciences, University of East Anglia, Norwich, NR4 7TJ U.K.

Received March 27, 1995; Revised Manuscript Received July 25, 1995®

ABSTRACT: Electronic absorption, MCD, and ^{1}H NMR spectroscopy have been used to characterize the structures and linkage relationships of three active site states, LS1, HS, and LS2, of the Trp51Ala variant of yeast cytochrome *c* peroxidase (C*c*P) in the Fe(III) state. In addition, the binding of three substrates (styrene, catechol, and guaiacol) to the Fe(III) variant has been studied by ^{1}H NMR spectroscopy, and the paramagnetically shifted resonances of the cyanide adduct of the variant have been assigned. The heme iron is hexacoordinated in all three pH-dependent states of the enzyme. LS1, the dominant acidic species, exhibits electronic and MCD spectra indicative of low-spin, bis-histidine coordination environment for the heme iron. The HS form, which dominates at intermediate pH, exhibits electronic, MCD, and ^{1}H NMR spectra characteristic of high-spin heme Fe(III) with axial histidyl and water ligands. The LS2 species exhibits spectroscopic properties indicative of a bis-histidine, low-spin Fe(III) derivative. The equilibrium constants for interconversion of these forms of the variant enzyme are highly dependent on ionic strength, specific anions, and temperature of the solution, with the HS form stabilized relative to the other forms in the presence of several noncoordinating, anionic species. Aromatic substrates such as styrene, catechol, and guaiacol affect the chemical shifts of the heme substituents of the HS species but not of the LS2 species. Based on these results, a model is proposed that accounts to a large extent for the electrostatic origin of the three forms of the active site of the Trp51Ala variant and the mechanisms by which they are differentially stabilized in solution.

The physiological activity of cytochrome *c* peroxidase (C*c*P) is the catalysis of ferrocytochrome *c* oxidation to ferricytochrome *c* by hydrogen peroxide (see review by Bosshard et al., 1990). In previous studies, the Trp51Ala variant of this enzyme was also shown to catalyze the oxidation of small organic substrates (Miller et al., 1992). As established by X-ray crystallographic studies (Finzel et al., 1984), Trp51 resides in the distal heme pocket with its indole ring oriented parallel to the plane of the heme prosthetic group (Figure 1). In addition, the indole nitrogen atom of Trp51 forms a hydrogen bond to one of three water molecules present in the distal heme pocket that form a hydrogen-bonding network with other residues present in this region of the protein. Despite the presence of these water molecules near the ligand binding site, the heme iron atom of resting state C*c*P remains predominantly pentacoordinate and high-spin between pH 4 and 8 (Vitello et al., 1990).

Replacement of Trp51 with an alanyl residue alters the heme building environment considerably and can be expected to alter the structural and functional properties of this enzyme significantly. It was, in fact, the potential creation of a cavity or putative substrate binding site by this substitution that led to the evaluation of small substrate oxidation by this variant in previous work (Miller et al., 1992). Although previous studies have provided initial characterization of the Trp51Ala variant (Goodin et al., 1991), detailed characterization of the coordination chemistry and the structural properties of the active site of this variant has not been reported. To address these issues, we have studied the pH-dependent properties of this variant by electronic, MCD, and ^{1}H NMR spectroscopy. In addition, we have studied the interaction of three

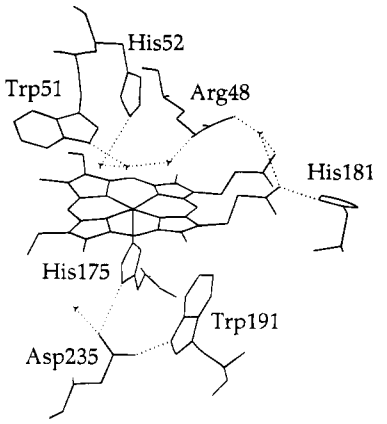

FIGURE 1: The active site of yeast cytochrome *c* peroxidase (prepared from the coordinates reported by Finzel et al., 1984).

† This research was supported by MRC Operating Grant MT-7182 (to A.G.M.), by Progetto Strategico Tecnologie Chimiche Innovative of the Italian CNR, by EC Biotechnology Program No. BIO2-CT94-2052 (DG12SSMA) (to I.B. and L.B.), and by a grant from the BBSRC (to A.J.T.).

‡ University of Florence.

§ University of British Columbia.

|| Present address: Departament de Bioquímica i Biologia Molecular, Facultat de Química, Universitat de Barcelona, Martí i Franqués, 1, 08028 Barcelona, Spain.

⊥ University of East Anglia.

® Abstract published in *Advance ACS Abstracts,* October 1, 1995.

0006-2960/95/0434-13895$09.00/0 © 1995 American Chemical Society

organic substrates with this enzyme by ^{1}H NMR spectroscopy.

EXPERIMENTAL PROCEDURES

Site-Directed Mutagenesis and Protein Expression and Purification. The mutant gene coding for the Trp51Ala variant of *Cc*P from baker's yeast reported previously (Goodin et al., 1991) was expressed in *Escherichia coli* using the expression system (Fitzgerald et al., 1994) recently employed for the production of the Asp235Ala variant (Ferrer et al., 1994). The first three amino acid residues at the amino terminus of both the wild-type and variant enzymes used here are Met-Lys-Thr rather than Thr-Thr-Pro that occur in the naturally-occurring wild-type form of the baker's yeast enzyme. In addition, Thr53 and Asp152 observed in the enzyme isolated from commercial baker's yeast (Finzel et al., 1984) have been introduced to replace Ile53 and Gly152 present in the cloned gene (Kaput et al., 1982) upon which the expression system is based. Crystals of the variant enzyme were prepared by the method used for the wild-type and the Asp235Ala variant enzymes (Ferrer et al., 1994).

Electronic Spectroscopy. Electronic absorption spectra were obtained with a Cary Model 219 spectrophotometer interfaced to a microcomputer (OLIS, Bogart, GA) and fitted with a Lauda Model RS3 circulating thermostated water bath and a jacketed cuvette holder. The spectrophotometric pH titrations were performed by dissolving the protein (ca. 10 μM) in the appropriate buffer and adjusting the pH with a concentrated solution of potassium hydroxide. Similarly, anion titrations were performed by successive additions of a concentrated solution (1 M) of the corresponding anion to a solution of the protein in 20 mM MOPS, pH 6.0.

MCD Spectroscopy. Magnetic circular dichroism spectra were measured in deuterated buffer solutions at the indicated pH, using an Oxford Instruments superconducting solenoid with a 25 mm room temperature bore capable of generating magnetic fields up to 6 T and either a Jasco J-500D circular dichrograph for the wavelength range 300−1000 nm or a home-built dichrograph (Gadsby & Thomson, 1990) for the range 800−2300 nm. Protein concentrations in the range 60−80 μM were used for data collection between 300 and 800 nm, while concentrations in the range 400−900 μM were used for collection of data between 800 and 2300 nm. In both cases, the optical path length was 1 mm.

NMR Spectroscopy. ^{1}H NMR spectra of the Trp51Ala variant and its derivatives (~2 mM) were recorded with Bruker MSL 200 and AMX 600 spectrometers. All spectra obtained at 200 MHZ resolution were collected with a superWEFT (water eliminated Fourier transform) (Inubushi & Becker, 1983) pulse sequence with a recycle delay of 120 and 200 ms for the native and cyanide inhibited species, respectively. The identification of the two nonexchangeable protons of the proximal histidine ring in the cyanide adduct of the Trp51Ala variant was achieved with the same pulse sequence with a recycle delay of 10 ms and a τ value of 5 ms. The ^{1}H nuclear Overhauser effect (NOE) experiments (at 200 and 600 MHz) were performed with the superWEFT pulse sequence for water signal suppression and were collected using the previously reported method (Unger et al., 1985; Banci et al., 1989). Difference spectra were collected by applying the decoupler frequency on- and off-resonance, alternately, according to the scheme ω, $\omega + \delta$, $\omega - \delta$, where ω is the frequency of the irradiated signal and δ is the offset for the off-resonance irradiation. The application of the off-resonance decoupling symmetrically on both sides of the saturated signal minimized the off-resonance effects in the saturation. The phase of the receiver was alternated accordingly, so that a difference free induction decay was collected directly. Nonselective T_1s were measured with the inversion recovery pulse sequence (Vold et al., 1968).

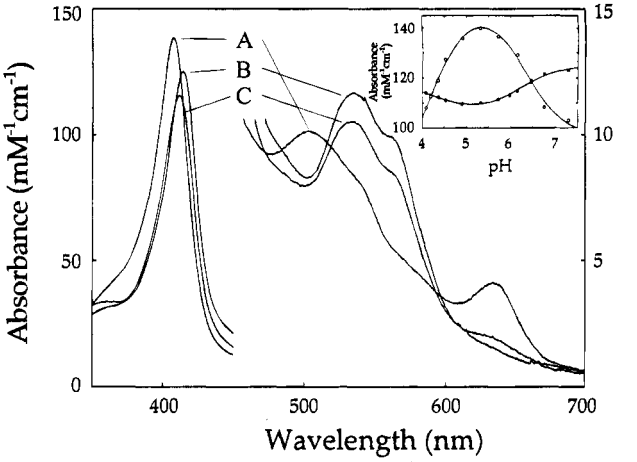

FIGURE 2: Electronic absorption spectra of Trp51Ala *Cc*P in 0.1 M KNO_3 (298 K) at selected pH: A, pH 5.3; B, pH 7.3; C, pH 4.1. Inset: pH dependence of the absorptivity at 407 nm (○) and 414 nm (●) of Trp51Ala *Cc*P in 0.1 M KNO_3 (298 K). The solid lines represent the nonlinear fits of these data to two single-proton processes with apparent pK_a of 4.3 ± 0.2 and 6.3 ± 0.2.

NOESY (Macura et al., 1982; Marion & Wüthrich, 1982), COSY (Bax et al., 1981; Bax & Freeman, 1981), and TOCSY (Bax & Davis, 1985) spectra at 295 and 288 K were recorded at 600 MHz using presaturation to eliminate the solvent signal. TPPI NOESY spectra were recorded at mixing times of 15 ms to avoid spin diffusion. A total of 512 spectra was collected with 1K data points in the *F*2 direction. The data were multiplied in both dimensions by a sine-squared bell window function with a phase shift of 45° and were zero-filled to obtain 1K × 1K real data points. COSY spectra consisting of 512 experiments with 1K data points in the *F*2 direction were processed in both dimensions by a pure sine-squared bell window function and zero-filled to obtain 1K × 1K real data points.

RESULTS

Electronic Spectroscopy. The Trp51Ala variant of *Cc*P in 0.1 M $NaNO_3$ exhibits two apparent spin transitions between pH 4 and 7.5 (Figure 2). At acidic pH, the predominant species exhibits an electronic spectrum indicative of a hexacoordinate, low-spin iron(III) derivative (LS1). The absorption maxima of this derivative (λ_{max} = 412, 534, and 563 nm) are consistent with a bis-histidyl coordination environment for the heme iron (Smulevich et al., 1991). At intermediate pH values, an electronic spectrum typical of a high-spin, six-coordinate heme iron(III)-containing species (HS, λ_{max} = 407, 504, 634 nm) is observed. At basic pH values, the electronic spectrum is characteristic of another low-spin derivative (LS2, λ_{max} = 414, 534, 562 nm) with bis-histidyl coordination. The pH-dependent changes in absorbance monitored (298 K) at the Soret maxima of the high-spin (λ_{max} = 407 nm) and low-spin (λ_{max} = 414 nm)

Table 1: Apparent pK_a of the Two pH-Dependent Spin Transitions of Trp51Ala CcP in Various Buffers (298 K)[a]

salt/buffer	LS1 ⇌ HS (pK_1)	HS ⇌ LS2 (pK_2)
10 mM $NaNO_3$	4.4	6.0
0.1 M $NaNO_3$	4.3	6.3
10 mM $NaClO_4$	ND	6.0
0.1 M $NaClO_4$	3.8	6.4
0.1 M NaP_i	3.7	7.1
0.1 M NaF	ND	7.0
0.1 M MES	5.0	6.6

[a] The standard error in all pK_a values is ±0.2; ND, not determined.

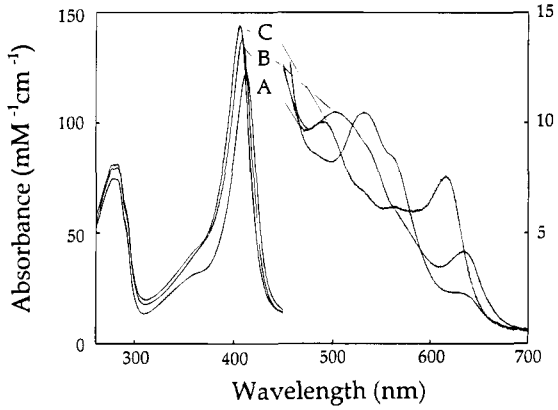

FIGURE 3: Electronic absorption spectra of Trp51Ala CcP in 20 mM MOPS, pH 6.0 (298 K), in the presence and absence of added Na_2SO_4 or NaF: A, no addition; B, Na_2SO_4 (80 mM); C, NaF (50 mM).

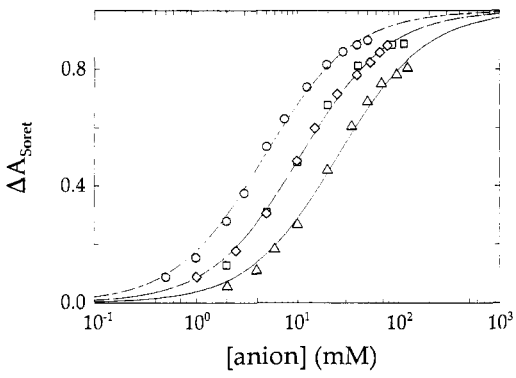

FIGURE 4: Anion binding isotherms of Trp51Ala CcP in 20 mM MOPS, pH 6.0 (298 K). Absorbance changes were monitored at the Soret maximum for the high-spin form and are normalized to a total absorbance change of 1.0. The lines represent the nonlinear fits of the data to binding isotherms for 1:1 ligand–protein complexes: NaF (○), Na_2SO_4 (□), $NaClO_4$ (◇), $NaNO_3$ (△).

species can be fitted to an equation describing two single proton titrations with pK_a values of 4.3 and 6.3 (Figure 2, inset). These pK_a values are strongly dependent on the buffer employed, its concentration, and specific anions that are present (Table 1).

Similarly, the addition of anions to a solution of Trp51Ala CcP in 20 mM MOPS, pH 6.0, conditions under which the variant protein is predominantly in the LS2 form, favors the conversion of the enzyme to the HS form (Figure 3). The data obtained from the titration of the enzyme with increasing concentrations of various anions are consistent with the formation of 1:1 complexes in all cases examined. The binding isotherms for the anions studied are shown in Figure 4, and the calculated apparent dissociation constants (K_d (mM)) for these complexes derived from these data were in

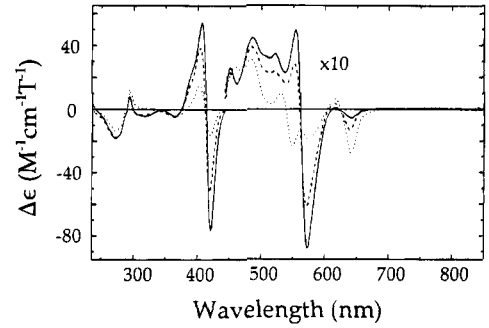

FIGURE 5: UV–visible MCD spectra of Trp51Ala CcP (ambient temperature). (- - -) 100 mM MES buffer, pH 3.6; (•••) 100 mM sodium phosphate buffer, pH 5.4; (—) 100 mM sodium phosphate buffer, pH 8.8.

the millimolar range, with nitrate having lower affinity than sulfate or perchlorate (pH 6.0, 20 mM MOPS buffer, 298 K): NO_3^-, 25 ± 5; SO_4^{2-}, 11 ± 3; ClO_4^-, 10 ± 2; F^-, 4.7 ± 0.5. The HS species obtained upon the addition of saturating concentrations of nitrate, sulfate, or perchlorate are spectroscopically indistinguishable from one another and are identical to that observed for the variant at low anion concentrations at pH ~5. These anions exhibit poor coordination properties and are not expected to bind to the heme iron.

On the other hand, addition of fluoride results in formation of an alternative high-spin species that is distinct from HS and that results from coordination of fluoride to the heme iron as observed for the wild-type enzyme (Edwards et al., 1984). Upon increasing the pH, the HS species formed in the presence of 0.1 M NaF also produces LS2 as observed in the presence of noncoordinating anions, but in this case the titration data could be fitted only with the assumption of a two-proton process (pK_a = 7.0; Table 1).

MCD Spectroscopy. The UV–visible MCD spectra of the Trp51Ala variant obtained at ambient temperature and three pH values are shown in Figure 5. Between 350 and 450 nm, the spectra of the variant exhibit features typical of the MCD Soret band of low-spin ferric heme, which is comprised of *C* terms of opposite sign (Vickery et al., 1976a). Peak-to-trough intensities for such bands are ~150 M^{-1} cm^{-1} T^{-1} and will dominate any contributions from high-spin ferric heme, which are much less intense, e.g., ~15 M^{-1} cm^{-1} T^{-1} for aquo metmyoglobin and ~6 M^{-1} cm^{-1} T^{-1} for the fluoride complex of metmyoglobin (Vickery et al., 1976b). The 450–600 nm region is also dominated by contributions from low-spin heme, which exhibits a dispersion-shaped MCD α-band of intensity +4 to −10 M^{-1} cm^{-1} T^{-1}. High-spin α-bands are blue-shifted and at least one-fifth as intense. The high-spin ferric "630 nm" band in the absorption spectrum appears in the MCD as a dispersion-shaped feature (Brill & Williams, 1961). The high-energy positive side of this feature is again lost under low-spin α-band intensity, but the lower energy negative component is observed at 640 nm. Such a band typically has an intensity of 3–4 M^{-1} cm^{-1} T^{-1}. The energy of this trough (640 nm) is typical for histidine/H_2O ligated ferric hemes such as observed in the case of wild-type myoglobin (Matsuoka et al., 1992). In the spectra of pentacoordinate histidine-bound hemes, such as native HRP, this band is shifted to ~660 nm (Nozawa et al., 1976; Kobayashi et al., 1977; Bracete et al., 1991).

The near-infrared MCD spectra of Trp51Ala at selected pH values and ambient temperature are shown in Figure 6.

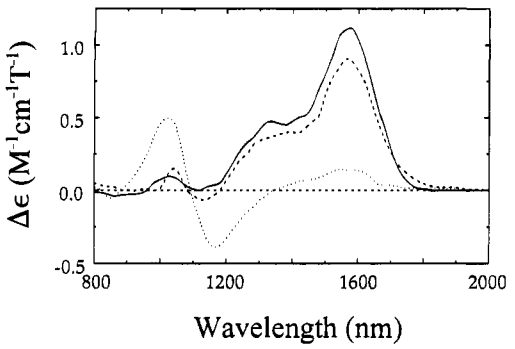

FIGURE 6: Near-infrared MCD spectra of Trp51Ala C*c*P (ambient temperature). (- - -) 100 mM MES buffer, pH 3.6; (•••) 100 mM NaP_i buffer, pH 5.4; (—) 100 mM NaP_i buffer, pH 8.8.

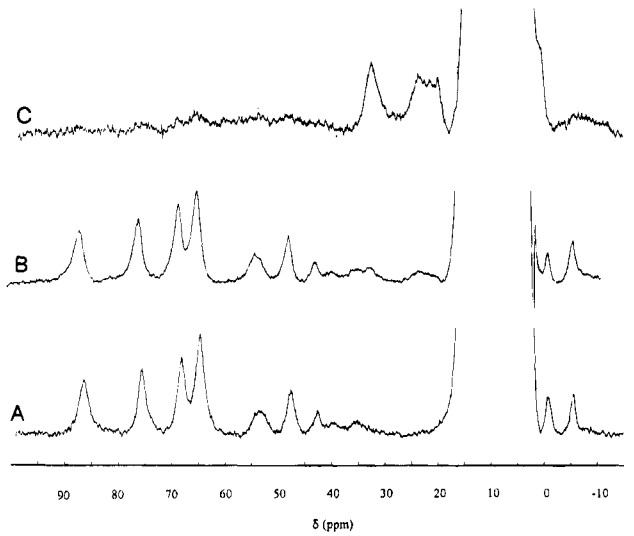

FIGURE 7: 200 MHz ^{1}H NMR spectra of the Trp51Ala variant (296 K, 0.1 M sodium phosphate buffer) at (A) pH 6.5, (B) 7.5, and (C) 8.3.

In this region, the spectrum exhibits a charge-transfer band from both high-spin and low-spin ferric heme. The low-spin band is positive and absorption shaped with a positive vibrational side band to higher energy (Cheesman et al., 1991). The absorption maximum of the main component is diagnostic of the axial ligands to the heme iron (Gadsby & Thomson, 1990). The absorption maximum observed at ~1580 nm is typical for bis-histidine ligation. The high-spin charge-transfer band also varies with ligation, but there are insufficient examples of such systems that have been characterized in this manner to permit construction of a complete spectroscopic scale. However, an absorption maximum near 1100 nm is known to be typical of histidine/water coordination, e.g., as seen for myoglobin at 1066 nm (Eglinton et al., 1983) and for hemoglobin at 1107 nm (Stephens et al., 1976). The pentacoordinate histidine-ligated heme systems that have been examined have this band at 1200 nm, e.g., HRP (Kobayashi et al., 1977), and between 1255 and 1285, e.g., cytochrome *c*′ (Rawlings et al., 1977).

^{1}H NMR Spectroscopy. The 200 MHz ^{1}H NMR spectra of the Trp51Ala variant at pH 6.5, 7.5, and 8.3 (296 K, 0.1 M phosphate buffer) are shown in Figure 7. The pH dependence of the ^{1}H NMR spectra is consistent with the equilibria observed by electronic spectroscopy over the same pH range. In the spectrum recorded in D_2O at pH 6.5, four resonances of integrated intensity three are observed at 81.9, 70.8, 63.3, and 59.9 ppm that can be attributed to the heme methyl protons of the high-spin form. Other resonances of intensity one are present in the near downfield region. The spectrum of this species is similar to that of wild-type C*c*P. The mean chemical shifts of the heme methyl groups have been determined in H_2O and D_2O for both the wild-type (H_2O, 70.4; D_2O, 71.0) and variant (H_2O, 69.7; D_2O 69.0) enzymes (100 mM sodium phosphate buffer, pH 6.5, 296 K). For the wild-type enzyme, $\%\Delta\delta$ [i.e., 100 × (the mean chemical shift observed in D_2O − the mean chemical shift observed in H_2O)/(the mean chemical shift observed in D_2O)] is 0.8, while this same value is −1.0 for the variant. In previous studies (La Mar et al., 1988; Rajarathnam et al., 1991), the value of $\%\Delta\delta$ has been related to isotope effects produced by different contact contributions to the hyperfine shifts that reflect the fact that the H-bond with the distal His residue is stronger in D_2O than in H_2O which, in turn, is consistent with the expectation that D_2O is a stronger ligand to the heme iron than H_2O. While this explanation provides no information concerning the sign of the expected isotope effect, differences in the ligand field are probably accompanied by distortion in the coordination geometry, which complicates the analysis. Nevertheless, in all reported examples of this type of analysis, the sign of the quantity $\%\Delta\delta$ is positive. Our observation of a negative value for the Trp51Ala variant suggests that this interpretation may require further investigation.

When the pH is increased to 7.6, two envelopes of signals in the 20−40 ppm range increase in intensity. At pH 8.3, the resonances shifted far downfield disappear while those in the 20−40 ppm range become the only features of the spectrum. The resonances in this range indicate the presence of a low-spin species (LS2) at pH >8. At pH 7.5 and 296 K the spectrum of the HS species dominates, while at pH 8.3, LS2 is the principal contributory species. This observation is consistent with a pK_a value of ~7.8 for the HS ⇌ LS2 equilibrium. This equilibrium is strongly dependent upon temperature (Figure 8). At pH 7, the spectrum recorded at 291 K is dominated by the HS species, while at 301 K only the LS2 form is present. Similar behavior has been reported previously for the Asp235Ala variant of this enzyme (Ferrer et al., 1994). The HS ⇌ LS2 equilibrium characterized by NMR spectroscopy is consistent with the results obtained by electronic spectroscopy. The difference in apparent pK_a values obtained for this equilibrium determined by the two spectroscopic methods suggests that the pK_a increases with the greater concentration of protein used for the NMR studies.

The T_1 value, measured at 200 MHz, of the heme methyl resonance at 27.5 ppm in the spectrum of the low-spin species (LS2) that dominates at pH 8.3 is about 48 ms (*vide infra*). This value is comparable to the T_1 values of the heme methyl resonances of cytochrome b_5 (42−67 ms) (McLachlan et al., 1988), which possesses bis-histidine coordination to the heme iron. On the other hand, this T_1 is much greater than those observed for the methyl resonances of alkaline metMb (1−2 ms) (Yamamoto, 1993), which possesses a $^-$HO−Fe−His coordination environment. When the dominant contribution to nuclear relaxation is the coupling between the resonating nucleus and the unpaired electron, the recovery of the magnetization after a nonselective excitation follows exponential behavior (Banci et al., 1991b; La Mar & de Ropp, 1993). Under these conditions, we can define as T_1 the time constant for this exponential process.

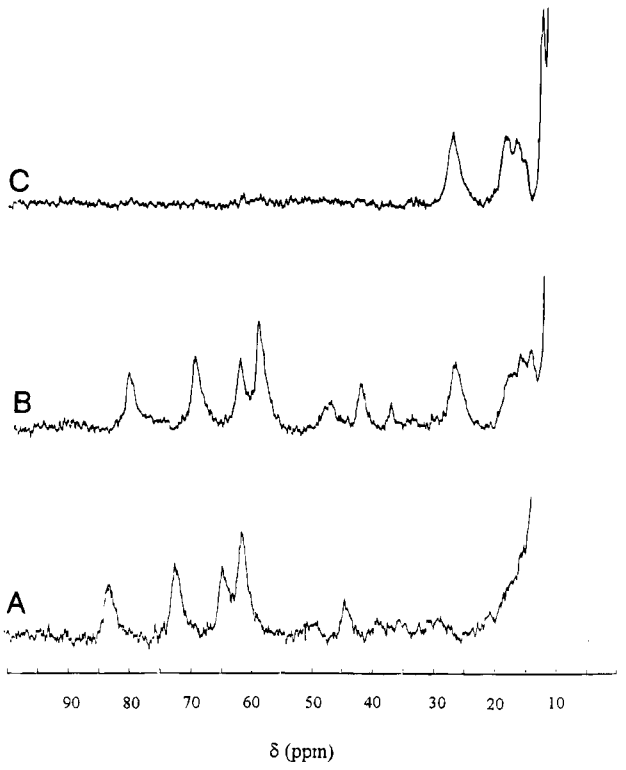

FIGURE 8: 200 MHz ^{1}H NMR spectra of the Trp51A variant (0.1 M sodium phosphate buffer, pH 7.0) at (A) 291 K, (B) 296 K, and (C) 301 K.

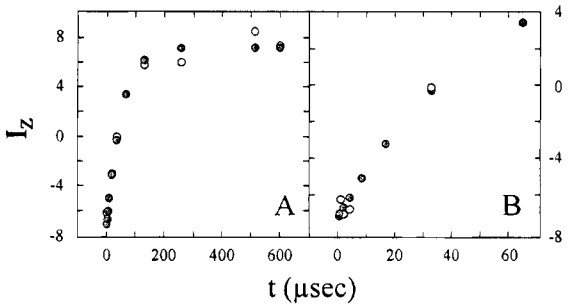

FIGURE 9: ^{1}H NMR experimental (○) and calculated (●) intensities I_z for the heme methyl resonance at 27.5 ppm of the LS2 species as a function of the delay times t (ms) between subsequent pulses in an inversion–recovery pulse sequence (0.1 M sodium phosphate buffer, pH 8.3, 296 K). The experimental data have been fitted to a single exponential. The panel on the left shows a fitting performed on the full time scale, while the panel on the right shows a fitting performed using only the initial part of the magnetization recovery curve.

When the contribution due to the resonating nucleus-unpaired electron coupling is sizable but not dominant, only the initial part of the magnetization recovery in a nonselective experiment provides the paramagnetic contribution to nuclear relaxation (Banci et al., 1991b; Banci, 1993; La Mar & de Ropp, 1993). In the present system, the heme methyl relaxation data can be fitted to a single exponential (Figure 9A). No difference is found between the analysis of the initial part of the magnetization recovery ($T_1 = 48.8 \pm 3.7$ ms) (Figure 9B) and that of the whole magnetization recovery curve ($T_1 = 47.8 \pm 2.5$ ms) (Figure 9A) within experimental error. This finding indicates that the relaxation rates are dominated by hyperfine coupling and, therefore, that the differences in T_1 values reflect differences in the electronic relaxation times (τ_s) of the iron, as the proton–metal distances for heme methyls are the same in all the systems. In turn, the τ_s values are determined by the electronic structure of the iron, which is related to the nature and the properties of its ligands. From the T_1 values, it is evident that the τ_s of the iron in the Trp51Ala variant should be much closer to that observed for cytochrome b_5 than that observed for metMb–OH, suggesting a coordination sphere in the variant that is similar to that of cytochrome b_5.

At the lowest pH value (4.5) at which the protein is stable at the concentrations required for ^{1}H NMR measurements, the LS1 species is not detected over the temperature range 281–301 K (data not shown). The LS1 species could, in principle, be studied in MES buffer where the LS1 ⇌ HS transition occurs with a pK_a ~5. However, the solubility of the protein in MES buffer is quite low and not sufficient to permit the detection of the hyperfine-shifted signals in the ^{1}H NMR spectrum.

^{1}H NMR Spectroscopy of the Cyanide Adduct. The 600 MHz ^{1}H NMR spectrum of the cyanide adduct of the Trp51Ala variant is shown in Figure 10 (0.1 M phosphate buffer, pH 7, 295 K). The hyperfine-shifted resonance assignments derived from a combination of 1D NOE and 2D COSY, TOCSY, and NOESY ^{1}H NMR experiments are reported in Table 2. The spectrum of this derivative is clearly very similar to that of the cyanide adduct of the wild-type enzyme (Table 2). Even the resonances of the distal histidine, which is adjacent to the tryptophanyl residue that is substituted in this variant, are not changed significantly. Interestingly, the exchangeable signal b, which we tentatively assigned in the spectrum of the wild-type cyanide adduct as arising from an NH proton of Arg48 (Banci et al., 1991a), is present in the spectrum of the Trp51Ala variant, at 18.8 ppm, thereby ruling out the alternative assignment of this resonance to the NH of the Trp51 indole ring (Satterlee & Erman, 1991).

Binding of Aromatic Molecules. The Trp51Ala variant was previously reported to bind some aromatic molecules (e.g., styrene and catechol) in the vicinity of the heme binding site with much greater affinity than that exhibited by the wild-type enzyme (Miller et al., 1992). As part of this study, therefore, it was of interest to characterize the interaction of these molecules with both the ligand-free and cyanide adduct of the variant enzyme by NMR spectroscopy.

Addition of styrene (65-fold molar excess) and catechol (100-fold molar excess) to the Trp51Ala variant at pH 6.5 (100 mM sodium phosphate buffer) produces NMR spectra that are nearly identical to each other. The principal effect observed is that the resonances of the four heme methyl groups are shifted by 1–4 ppm (data not shown). Addition of guaiacol up to a 40-fold molar excess produces minor effects that are similar to those produced by addition of the other two molecules, while further addition of guaiacol results in the disappearance of all of the isotropically shifted signals. The exchange between the bound and unbound forms of the protein is fast on the NMR time scale at 200 MHz (data not shown). No further spectroscopic changes are observed at higher concentrations of any of these substrates.

When pH is increased, the spectra of the styrene and catechol adducts convert to that of the substrate-free form, LS2. For the styrene adduct, an apparent pK_a ~8.2 is estimated; i.e., this pK_a is greater than observed in the unbound form of the enzyme. In contrast, the binding of

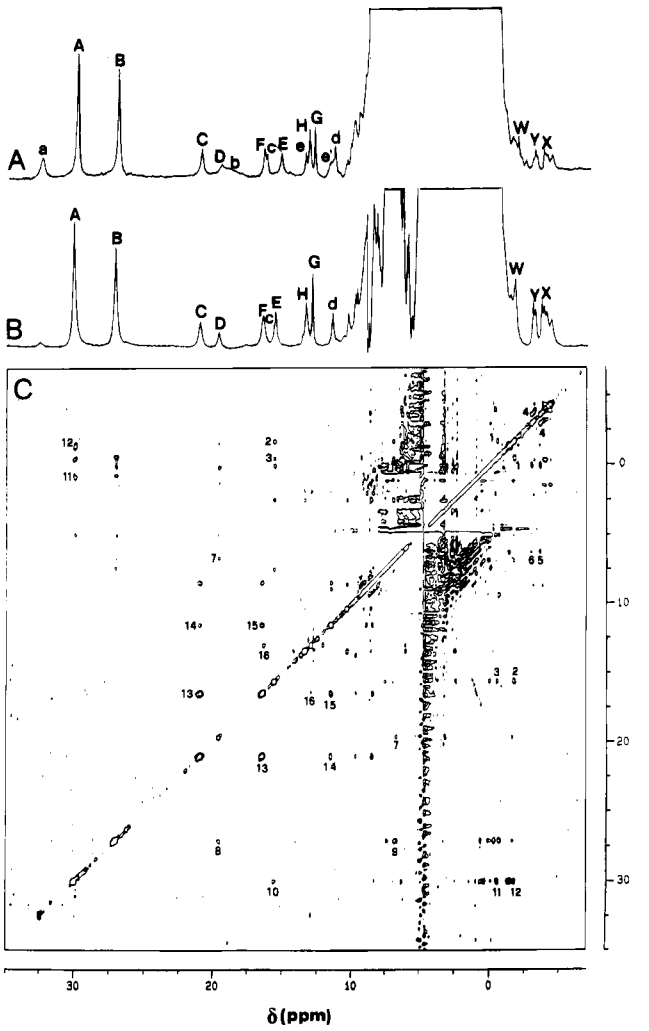

FIGURE 10: 600 MHz ^{1}H NMR spectra of the cyanide adduct of Trp51Ala *Cc*P (0.1 M phosphate buffer, pH 7, 295 K): (A) 1D spectrum in H_2O; (B) 1D spectrum in D_2O. The labeling of the signals is the same as in Table 2. (C) TPPI NOESY map in D_2O recorded with a mixing time of 15 ms. Cross peak assignments are as follows: (1) 4-Hβ_{cis}, 4-Hβ_{trans}; (2) 4-H, 4-Hβ_{cis}; (3) 4-H, 4-Hβ_{trans}; (4) 2-Hβ_{cis}, 2-Hβ_{trans}; (5) 2-H, 2-Hβ_{cis}; (6) 2-H; 2-Hβ_{trans}; (7) 7-H, 7-H′; (8) 8-CH_3, 7-H; (9) 8-CH_3, 7-H′; (10) 3-CH_3, 4-H; (11) 3-CH_3, 4-Hβ_{trans}; (12) 3-CH_3, 4-Hβ_{cis}; (13) Hβ His175; Hβ′ His175; (14) Hβ His175, NH_p His175; (15) Hβ′ His175, NH_p His175; (16) H1 His52, H1 His52; (17) H2 His52, H1 His52. Cross peaks 8 and 10 are better detected using different processing conditions. Connectivities involving the exchangeable resonances a, c, and d are detected also in the NOESY map recorded in D_2O since the mentioned signals are exchanging slowly (see the comparison of the spectra reported in traces A and B).

catechol to the enzyme decreases this pK_a to ~7. When styrene and catechol are added to the variant at pH 8.3, no change in the NMR spectrum is observed. Greater concentrations of styrene are required to produce the appearance of small quantities of the high-spin, substrate-bound form of the enzyme similar to that observed at pH 6.5.

To obtain greater insight into the nature of the substrate-bound forms of the enzyme, formation of these adducts was studied by titrations monitored by CD and electronic spectroscopy (data not shown). No significant changes were detected in the 400−800 nm region at pH 6.5 upon addition of either styrene or catechol, suggesting that no perturbation in the coordination sphere of the heme iron is produced.

We have also characterized the adducts of these aromatic molecules with the cyanide adduct of the Trp51Ala variant

Table 2: ^{1}H NMR Chemical Shift Values for the Hyperfine-Shifted Signals of the Cyanide Adducts of Wild-Type *Cc*P[a] (301 K), the Trp51Ala *Cc*P Variant (295 K), and the Trp51Ala−Styrene Species (295 K)

assignment	wild-type	Trp51Ala	Trp51Ala−styrene	signal
heme				
2Hα	7.1	6.3	6.8	J
2Hβ*trans*	−3.0	−2.9	−3.5	Y
2Hβ*cis*	−3.7	−3.6	−4.2	X
3-CH_3	30.6	29.9	29.9	A
4Hα	16.0	15.4	14.4	E
4Hβ*trans*	−2.1	−0.5	−1.2	V
4Hβ*cis*	−3.8	−1.6	−2.8	W
7Hα	18.3	19.5	18.5	D
7Hα′	6.4	6.8	6.8	I
8-CH_3	27.6	26.9	25.2	B
distal His				
Hδ1	16.5	16.4	16.5	c
Hϵ1	14.0	13.0	13.6	G
Hδ2		13.6	12.0	H
Hϵ2	28.4	31.5	34.6	a
proximal His				
NH_p	12.9	11.4	13.0	d
Hβ	19.4	20.9	19.6	C
Hβ′	14.8	16.5	15.5	F
Hδ1	10.2	10.1		f
Hϵ1	−20.6	−23.6	−20.1	Z
Hδ2	15.8	18.7		H′

[a] Banci et al., 1991a,b.

by ^{1}H NMR. Indeed, we can take advantage of the assignment of the hyperfine-shifted signal of this species to obtain information on the binding mode of the aromatic molecules. For binding of all three substrates, exchange with unbound substrate is semi-slow on the 600 MHz ^{1}H NMR time scale. When ~50% of the substrate-bound adduct is formed, broadening of the hyperfine-shifted signals is observed. When all of the variant enzyme is saturated with substrate, most of the signals become sharp again (Figure 11). Moreover, the binding of each of the aromatic molecules to the variant enzyme affects the ^{1}H NMR spectrum of the enzyme differently (Figure 11). In the case of styrene, the affinity is relatively high, and the enzyme is fully bound with substrate at a styrene/enzyme molar ratio of ~50. From the NOESY spectrum of this adduct, unambiguous assignments of the hyperfine-shifted signals can be obtained (Table 2). It can be seen that while the 3-CH_3 signal is essentially unaffected by the binding of styrene, the 8-CH_3 resonance is shifted upfield ~1.7 ppm and broadens by ~70 Hz (Figure 11). Furthermore, the signals of the proximal and distal histidines are also affected. For example, the Hϵ1 of the proximal His175 residue (Z) is shifted downfield by 3.5 ppm, while the Hϵ1 of the distal His52 (G) is shifted downfield by 0.6 ppm. Unfortunately, the very low solubility of styrene in water prevents observation of the NMR resonances of unbound styrene. This characteristic prevented us from performing NOE experiments to detect connectivities between the styrene and the protein protons.

The spectrum of the variant saturated with catechol has been obtained for a catechol/protein molar ratio of ~90. The 3-CH_3 resonance is shifted downfield by 0.6 ppm and broadened by 70 Hz upon catechol binding, while the 8-CH_3 resonance is essentially unchanged (Figure 11). This behavior of the methyl groups is opposite to that observed for styrene binding. Upon catechol binding, the resonances associated with the proximal histidine are not significantly

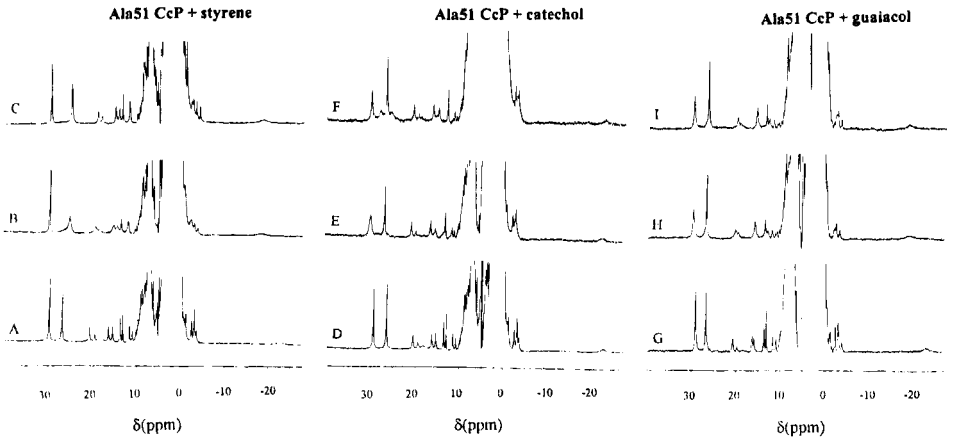

FIGURE 11: 600 MHz ^{1}H NMR spectra of the cyanide adduct of Trp51Ala CcP (0.1 M phosphate buffer, pH 7, D_2O, 295 K) upon titration with styrene (left), catechol (middle), and guaiacol (right). (A) Trp51Ala CcP−CN^-; (B) Trp51Ala CcP−CN^-/styrene molar ratio 1/25; (C) Trp51Ala CcP−CN^-/styrene molar ratio 1/50; (D) Trp51Ala CcP−CN^-; (E) Trp51Ala CCP−CN^-/catechol molar ratio 1/25; (F) Trp51Ala CcP−CN^-/catechol molar ratio 1/90; (G) Trp51Ala CcP−CN^-; (H) Trp51Ala CcP−CN^-/guaiacol molar ratio 1/40; (I) Trp51Ala CcP−CN^-/guaiacol molar ratio 1/80.

affected, while those of the distal histidine are perturbed. Notably, in the spectra obtained for the variant in water, the exchangeable signal a broadens beyond detection in the presence of catechol (data not shown).

Finally, addition of guaiacol produces small changes in the signals resulting from the 3-CH_3 and 8-CH_3 groups (Figure 11). The former is shifted 0.6 ppm downfield and broadened by 60 Hz, while the latter is shifted 0.3 ppm upfield and broadened by 10 Hz. Again, considerable variations are observed in the signals of the distal and proximal His residues (for example, signal Z is shifted 4.3 ppm downfield). The complexes formed by both catechol and guaiacol with the variant peroxidase are relatively unstable, and their NMR spectra change with time. Consequently, we were unable to obtain complete assignments of the spectra for these complexes.

DISCUSSION

The distal heme pocket of wild-type CcP is characterized by a network of hydrogen bonding interactions that stabilizes a remarkable solvent channel through suspension of three water molecules just above the plane of the heme prosthetic group (Figure 1). Interestingly, none of these water molecules coordinates to the heme iron (Finzel et al., 1984), and the CcP iron center is predominantly five coordinate over a relatively wide range of pH (Vitello et al., 1990). While the presence of a distal His residue would normally be expected to stabilize a distally-coordinated water molecule in the Fe(III) form of the enzyme, as observed for myoglobin and hemoglobin, the hydrogen bonding network provides alternative stabilizing interactions for the potential water ligand that prevent its coordination. Remarkably, replacement of Asp235 on the proximal side of the heme with either Asn (Smulevich et al., 1988; Satterlee et al., 1990; Vitello et al., 1992) or Ala (Ferrer et al., 1994) can also destabilize this distal hydrogen bonding network, presumably by altering the geometry and electronic properties of the heme iron. Previous studies indicated that variants of CcP in which Trp51 is substituted by a variety of amino acid residues suffer disruption of the hydrogen bonding network to produce forms of the enzyme that are hexacoordinate (Goodin et al., 1991) and that exhibit altered activity and pH dependences. This earlier work, however, did not define the coordination environments of these enzymes in detail or evaluate the manner in which they are influenced by pH and anion binding. The present study provides this characterization for the Trp51Ala variant through the combined use of electronic, NMR, and MCD spectroscopy. This variant was of particular interest owing to its ability to oxidize styrene, catechol, and guaiacol (Miller et al., 1992). Consequently, the present work includes initial investigation of the interaction of these organic substrates through use of ^{1}H NMR spectroscopy.

pH-Linked Forms of the Trp51Ala Variant. The Trp51Ala variant of CcP exhibits three spectroscopically distinct species between pH 4 and 7.5 that interconvert with apparent pK_a values that depend on the ionic composition of the solution. The neutral form, at intermediate pH, exhibits an electronic spectrum characteristic of high-spin Fe(III). Several features of the electronic spectrum of wild-type CcP and its variants have been shown to provide reliable information about the coordination state of the high-spin iron. Thus, pentacoordinate, high-spin forms exhibit a prominent shoulder (the δ band) near 380 nm, a charge-transfer band (CT) >640 nm, and relatively small A_{Soret}/A_{380} and $A_{620}/A_{CT\ band}$ ratios. The opposite is true for hexacoordinate forms of this protein (Vitello et al., 1992; Erman et al., 1993). At pH 5.3 in 0.1 M $NaNO_3$, conditions under which the relative concentration of the HS form of Trp51Ala is maximal (Figure 2), the A_{Soret}/A_{380} and $A_{620}/A_{CT\ band}$ ratios are 2.49 and 1.12, respectively, for the variant, while the corresponding values for the wild-type enzyme are 1.51 and 0.73 (Vitello et al., 1990). The CT band of the Trp51Ala variant occurs at 634 nm, which is blue-shifted 12 nm from that of the wild type enzyme. These observations indicate that the HS form of the variant enzyme is predominantly hexacoordinate. This conclusion is supported by the room temperature MCD spectrum of the protein at pH 5.4, which is consistent with the presence of a water molecule as the sixth axial ligand to the heme iron. Finally, the ^{1}H NMR spectrum of the HS form present at pH 6.5 is similar to that of wild-type CcP, albeit with some slight variations in chemical shifts.

As the pH is increased above pH 6, the electronic spectrum of Trp51Ala changes to that of a hexacoordinate, low-spin form (Figure 2), consistent with related analysis of other CcP variants (Smulevich et al., 1991). In addition, the room

temperature MCD spectrum recorded at pH 8.8 clearly indicates the presence of bis-histidine coordination in this form of the enzyme. From these results, we conclude that the distal histidine is coordinated to the heme iron under these solution conditions. Other *Cc*P variants with substitutions in the distal side of the heme pocket have been suggested to exhibit similar coordination behavior on the basis of electronic spectroscopy (Vitello et al., 1993).

The pH dependence of the electronic spectrum of Trp51Ala in the alkaline region (Figure 3) is consistent with the titration of a single ionizable group in the enzyme that controls the conversion between the neutral (HS) and basic (LS2) forms of this variant. The observation of a bis-histidine derivative (LS1) at acidic pH is an observation unique to the Trp51Ala variant. The identity of the axial ligands in this LS1 derivative has been established by electronic and room temperature MCD spectroscopy. As in the case of LS2, the sixth ligand to the heme iron must be the side chain of the distal histidine, and the observed pH-dependent changes are consistent with a single-proton process.

Effects of Noncoordinating Anions. The spectroscopic and functional properties of wild-type *Cc*P (Vitello et al., 1990) and several variants (Vitello et al., 1992, 1993; Erman et al., 1993; Ferrer et al., 1994) have been shown previously to be sensitive to the ionic composition of the solution. This effect has been attributed to the presence of an anion binding site in proximity to the heme pocket. The nature of the bound anionic species and the degree of occupancy of this binding site both have an effect on the properties of the enzyme. Furthermore, it has been shown that Arg48 in wild-type *Cc*P is responsible for nitrate binding in the heme pocket (Vitello et al., 1993). The direct consequence of the presence of an anion bound to Arg48, near His52 in the distal side of the heme pocket, presumably close to the structurally-linked titrating group in the heme pocket, is the electrostatic stabilization of the acidic form of this residue.

In the case of the Trp51Ala variant, the apparent pK_a of the HS $\rightleftharpoons$ LS2 transition increases with the concentration of anion (Table 1). Furthermore, conversion of LS2 to HS in this variant can be induced by the addition of anions to a buffered solution of the protein kept a constant pH (Figures 3 and 4). The binding data are consistent with formation of 1:1 complexes, and in the case of nitrate, perchlorate, and sulfate, the HS species formed upon anion binding are spectroscopically indistinguishable from each other and from HS formed in the absence of anions. This observation indicates that the anions that induce this conversion are not bound directly to the heme iron.

Other anionic species such as citrate, propionate, and *p*-toluenesulfonate (data not shown) are also capable of inducing this LS2 to HS transition. In contrast, the high-spin species formed on addition of fluoride differs from those formed by the other anions (Soret maximum = 405 nm, and CT maximum = 616 nm; Figure 3) and exhibits a spectrum similar to that reported for the fluoride complex of wild-type *Cc*P (Yonetani & Anni, 1987), in which the fluoride provides the distal ligand to the heme iron (Edwards et al., 1984). Nevertheless, increasing the pH of a solution of the fluoride complex of the Trp51Ala variant also leads to the formation of the LS2 form of the enzyme, indicating that at alkaline pH the fluoride is replaced by the distal histidine as the sixth ligand.

The results of the anion binding titrations (Figure 4) demonstrate that the HS form of Trp51Ala *Cc*P enzyme is stabilized by the presence of noncoordinating anions. For a given ionic strength, the pH range over which the variant protein remains in the HS form is greater for anions that exhibit greater affinity for the binding site in this enzyme (e.g., ClO_4^- vs NO_3^-). For a given anion, the range of pH over which the HS form of the protein is stable increases with the concentration of the anion (e.g., 100 mM vs 10 mM). This observation strongly suggests that one of the effects of anion binding to the variant enzyme is the electrostatic stabilization of the acidic form of the structurally-linked titratable group and that the protonation status of this residue is correlated with the spin and ligation state of the heme iron. Of all the noncoordinating anions examined, phosphate provides the greatest range of pH over which the HS form of the variant is stable (Table 1). This observation in turn suggests that phosphate has the greatest affinity for the anion binding site of this enzyme.

In the presence of phosphate, the wild-type enzyme exhibits an electronic absorption spectrum and reactivity with hydrogen peroxide that are essentially independent of pH (Vitello et al., 1990). This observation could be explained if (a) binding of anions to wild-type *Cc*P renders the behavior of the enzyme independent of pH and (b) phosphate binds with sufficient affinity that it can saturate the anion binding site at any pH between 4 and 8 if the phosphate concentration is 0.1 M. The pH-dependent properties observed in nitrate-containing buffers could then be explained in two alternative ways: (a) the anion-free enzyme exhibits pH-dependent properties and the lower affinity of the enzyme for nitrate (relative to phosphate) results in a fraction of the enzyme occurring in the anion-free form in 0.1 M nitrate; alternatively, (b) both forms of the protein, nitrate-bound and anion-free, could have pH-independent properties that are slightly different from each other, so that the observed pH-dependent changes result from a varying degree of occupancy of the anion binding site with pH.

Addition of cyanide to either the wild-type or variant enzymes results in quantitative formation of the hexacoordinate, cyanide-bound forms of the enzymes in which the bound cyanide is hydrogen bonded to the protonated imidazole of the distal His52 residue. The electronic and ^1H NMR spectra of the cyanide adduct of the Trp51Ala variant are quite similar to the corresponding spectra of the wild-type enzyme and Asp235Ala variant. Evidently, cyanide binding results in equivalent active site structures for all three forms of the enzyme.

Mechanism of the pH-Linked Structural Changes of the Trp51Ala Variant. The simplest explanation for the HS $\rightleftharpoons$ LS2 transition is that the distal His residue is the structurally-linked titratable group. In this model, the N^{ϵ} atom of the His 52 imidazole side chain would be protonated and positively charged at neutral pH and would, therefore, be unable to coordinate to the heme iron. Upon deprotonation of this side chain, His52 could bind to the heme iron. In this case, the observed pK_a for the HS $\rightleftharpoons$ LS2 transition would be attributable to the titration of the His52 side chain. However, the titration of the high-spin fluoride-bound derivative argues against this mechanism, because it involves a two-proton process while similar titrations performed in the presence of other noncoordinating anions are single-proton processes.

It is well-known that CcP binds moderately basic ligands such as fluoride, azide, and cyanide in their neutral forms (Erman, 1974). The proton that binds concomitantly with these anions protonates His52 (Banci et al., 1991a,b) and is involved in hydrogen bond formation with the coordinated anion. One of the two protons released in the pH titration of the fluoride derivative of the Trp51Ala variant upon formation of LS2 must derive from His52 because this residue must be deprotonated to coordinate to the heme iron. It is, therefore, reasonable to assume that the second proton is released by the structurally-linked group that controls the ligation status of the heme iron in this variant. The fact that the pH titration of the unligated HS form of the Trp51Ala variant is a single-proton process indicates that His52 is deprotonated in the HS form of the variant and that this residue does not control the HS ⇌ LS2 equilibrium. The titratable residue that is linked to the coordination state of the heme iron must reside near Arg48 because the pK_a for the HS ⇌ LS2 transition is highly sensitive to the identity of the anion bound at this presumed anion binding site. From examination of the three-dimensional structure of CcP, we propose that His181 is the residue that controls the transition between these two forms of the variant. His181 normally forms a hydrogen bond to the 7-propionate group of the heme, which in turn forms a hydrogen bond with the guanidinium group of Arg48 through a water molecule (Finzel et al., 1984; Edwards & Poulos, 1990). The small distance between the side chain of His181 and the anion binding site near Arg48 is consistent with the electrostatic stabilization of the protonated, positively charged form of His181 in the presence of anions. The exact mechanism by which deprotonation of His181 disrupts the hydrogen bonding network in which it is involved to increase the flexibility of the distal heme binding pocket is not clear. The net result of this process, nevertheless, is a local conformational rearrangement that leads to the collapse of the distal heme cavity and ligation of the distal His52 residue to the heme iron.

A pH-dependent transition of the visible absorption spectrum coupled with the concomitant release of two protons with a pK_a of 7.5 has been reported for ferrous wild-type CcP. This spectroscopic transition was ascribed to the change from a high-spin state to a slow-spin state that results from ligation of the distal His52 residue to the heme iron (Conroy et al., 1978). Similarly, infrared spectroscopy has been used to identify a two-proton process with a pK_a of 7.5 that corresponds to interconversion between low and high pH forms of the carbonyl derivative of Fe(II)−CcP (Iizuka et al., 1985). In this study, it was proposed that the high pH form represents a less rigid conformation of the protein. More recently, Edwards and Poulos (1990) suggested that His181 is one of the groups that titrates in the interconversion of these two forms of the enzyme and that the disruption of the hydrogen bonding network in which His181 is involved is the cause of the increased flexibility of the high pH form of the protein. The somewhat lower pK_a values for the HS ⇌ LS2 transition observed in the ferric form of the Trp51Ala variant could result from the excess charge carried by the iron in this form of the enzyme. Alternatively, the lower pK_a could result from the increased tendency of the variant to form the low-spin bis-histidine derivative LS2, presumably as the result of greater flexibility of the distal heme pocket that results from replacing Trp51 with an alanyl residue.

The HS → LS1 transition involves the protonation of a single titratable group that leads, again, to the coordination of His52 to the heme iron. We tentatively assign the identity of this titratable group to Asp235. Asp235 is located in the proximal heme pocket and forms hydrogen bonds with both the proximal His175 residue and with Trp191, the indole ring of which is in van der Waals contact with His175. Protonation of Asp235 would disrupt the hydrogen bond formed with these two residues, thereby reducing charge donation of His175 to the heme iron and increasing its acidity. The presumed greater flexibility of the distal heme binding pocket resulting from the mutation should favor the structural rearrangement required for coordination of His52 to the heme iron at low pH. In this case, the stabilizing effect of anion binding on the HS form of the protein cannot be easily explained through electrostatic effects. Instead, it seems likely that the more extended conformation of the HS form of the variant presents a greater affinity for anions than does the corresponding, more closed LS1 form. The HS and LS2 forms of the protein differ correspondingly in their relative affinities for small organic molecules.

Binding of Organic Molecules to the Trp51Ala Variant. Replacement of Trp51 with an alanyl residue potentially increases the accessible volume present at the base of the solvent channel that provides substrate access to the distal heme binding pocket. This stereochemical alteration in the distal heme pocket may permit the variant enzyme to bind small aromatic molecules that are not bound by the wild-type enzyme. As previously reported (Miller et al., 1992), aromatic molecules bound to the Trp51Ala variant in this manner can accept one oxygen atom from the ferryl group that is formed upon addition of hydrogen peroxide to the enzyme. From inspection of the three-dimensional structure of wild-type CcP (Finzel et al., 1984), it is apparent that the aromatic rings of these "pseudo"-substrate molecules could be located approximately in the same position as the six-membered ring of Trp51. Nevertheless, the substituents of the aromatic rings of these substrates have different properties. In styrene there is a hydrophobic vinyl group, and catechol is characterized by the presence of two hydrophilic phenolic OH groups.

On the basis of this observation, we suggest that these two molecules are oriented differently in the distal cavity. Specifically, the hydrophobic vinyl of styrene may be oriented toward the outside of the heme binding pocket, while the hydrophilic phenolic groups of the catechol may orient toward the hydrophilic region of the distal heme binding cavity, which is constituted by the distal His52 and Arg48. These differences in binding orientation could affect the extensive hydrogen bonding network present in the distal cavity differently and thereby account for the difference in pK_a values observed for the high spin−low spin transition. The differences in orientation of styrene, catechol, and guaiacol are also consistent with the results obtained for the cyanide adduct of the variant. Binding of styrene affects the chemical shift of the 8-CH_3 group more than does the binding of catechol or guaiacol, while the binding of catechol and guaiacol primarily affects the chemical shift of the 3-CH_3 group. Other binding-linked changes occur in the chemical shifts of the proximal and distal His protons. The latter can be accounted for by minor variations in the χ tensor and/or spin density pattern on the proximal His residue that result from structural rearrangements that occur when the substrate

enters the heme binding cavity. The broadening of the resonances can be attributed to the exchange of the aromatic molecules between two or more minima of the potential energy for binding in the distal heme pocket. These aromatic molecules do not bind to the Trp51Ala variant at high pH where the low-spin species is dominant. This observation is consistent with the suggestion that at alkaline pH the distal His residue is bound to the heme iron and the space available in the distal heme pocket is drastically reduced as a result.

Overview. Replacement of Trp51 with an alanyl residue disrupts the stability of the hydrogen bonding network in the distal heme pocket of *Cc*P to produce a facile equilibrium of three active site species: LS1, HS, and LS2. The distribution between these three forms is a function of pH and anion binding. The form observed at intermediate pH (HS) has been studied previously (Goodin et al., 1991) and has been suggested to be high-spin and hexacoordinate, with a distally bound water molecule. This suggestion has been confirmed in the present study by more detailed consideration of the visible electronic spectrum and by MCD spectroscopy. The form observed at high pH (LS2) exhibits electronic spectra and MCD spectra that are characteristic of low-spin, bis-histidine coordination. Alkaline forms of other *Cc*P variants have been suggested to possess this coordination environment (e.g., Asp235Asn, Vitello et al., 1992; Asp235Ala, Ferrer et al., 1994), but the MCD data reported in the current study together with the T_1 values of the heme methyl ^{1}H NMR resonances provide the most compelling evidence currently available for the existence of such a species. The Trp51Ala variant exhibits an unusually low pK_a for the formation of LS2 relative to other variants that exhibit LS2-type species. The binding of noncoordinating anions near Arg48, in the vicinity of His52, stabilizes the HS species of the variant. However, LS1, which is dominant at low pH, is the most surprising of the three forms because it exhibits bis-histidine axial ligation, verified by NIR-MCD spectroscopy, at acidic pH. This behavior is in contrast to that of other conformationally facile variants studied previously.

The manner in which these three forms of the variant interconvert and are affected by anion binding merits some speculation. We propose that the distal His52 residue remains in its neutral, unprotonated form over the pH range studied here. In the HS species, favored at intermediate pH, the distal heme ligand is a water molecule, which presumably forms a hydrogen bond with His52. As the pH is decreased, we propose that Asp235 becomes protonated and that the Asp235−His175 hydrogen bond is consequently disrupted. Loss of this hydrogen bond decreases the charge donation of the proximal His175 ligand to the heme iron, which increases the acidity of the iron atom, thereby promoting the deprotonation of the distal His52 and its coordination to the heme iron. The conversion of HS to LS2 involves the release of a single proton from a titratable residue that occurs concomitantly with coordination of His52 to the heme iron in LS2. We propose that this titratable residue is His181. The stabilization of the HS form by anion binding results from the proximity of the anion binding site near Arg48 (Vitello et al., 1993) to His181. The protonated, positively charged imidazole side chain of His181 favors formation of HS and is electrostatically stabilized by anion binding nearby. At all values of pH, the variant is less active than the wild-type enzyme (Goodin et al., 1991), presumably because the variant remains hexacoordinate over the pH range studied (3.5−8.7).

Although the Asp235Asn and Asp235Ala variants also exhibit three pH-linked, interconverting forms, the electrostatic properties of these forms of these variants differ considerably from those of the Trp51Ala variant. With the position 235 variants, the HS species predominates at low pH, and as the pH is increased, two low-spin forms, LS1 ($^-$HO−Fe−His) and LS2 (His−Fe−His), are formed successively as the pH is raised. Clearly, the architecture of the extensive hydrogen bonding interactions at the active site of *Cc*P responds in a complex and currently unpredictable manner to substitutions of amino acid residues that normally contribute to these stabilizing interactions. Only through the systematic, multidisciplinary characterization of variants such as that undertaken here will we eventually gain the insight necessary to understand the structural requirements for maintenance of such an extensive, internal hydrophilic protein environment.

ACKNOWLEDGMENT

We thank Dr. Bhavini Sishta for initial studies concerning structural variability of the active site of the Trp51Ala variant and its response to noncoordinating anions.

REFERENCES

Banci, L. (1993) in *Biological Magnetic Resonance* (Berliner, L. J., & Reuben, J., Eds.) Vol. 12, pp 79−111, Plenum Press, New York.

Banci, L., Bertini, I., Luchinat, C., Piccioli, M., Scozzafava, A., & Turano, P. (1989) *Inorg. Chem. 28*, 4650−4656.

Banci, L., Bertini, I., Turano, P., Ferrer, J. C., & Mauk, A. G. (1991a) *Inorg. Chem. 30*, 4510−4516.

Banci, L., Bertini, I., & Luchinat, C. (1991b) *Nuclear and Electron Relaxation. The magnetic nucleus-unpaired electron coupling in solution*, VCH, Weinheim.

Bax, A., & Freeman, R. (1981) *J. Magn. Reson. 44*, 542−561.

Bax, A., & Davis, D. G. (1985) *J. Magn. Reson. 65*, 355−360.

Bax, A., Freeman, R., & Morris, G. (1981) *J. Magn. Reson. 42*, 164−168.

Bosshard, H. R., Anni, H., & Yonetani, T. (1990) in *Peroxidases in Chemistry and Biology* (Everse, J., Everse, K. E., & Grisham, M. B., Eds.) Vol. II, pp 51−84, CRC, Boca Raton, FL.

Bracete, A. M., Sono, M., & Dawson, J. H. (1991) *Biochim. Biophys. Acta 1080*, 264−270.

Brill, A. S., & Williams, R. J. P. (1961) *Biochem. J. 78*, 246−253.

Cheesman, M. R., Greenwood, C., & Thomson, A. J. (1991) *Adv. Inorg. Chem. 36*, 201−255.

Conroy, C. W., Tyma, P., Daum, P. H., & Erman, J. E. (1978) *Biochim. Biophys. Acta 537*, 62−69.

Edwards, S. L., & Poulos, T. L. (1990) *J. Biol. Chem. 265*, 2588−2595.

Edwards, S. L., Poulos, T. L., & Kraut, J. (1984) *J. Biol. Chem. 259*, 12984−12988.

Eglinton, D. G., Gadsby, P. M. A., Sievers, G., Peterson, J., & Thomson, A. J. (1983) *Biochim. Biophys. Acta 742*, 648−658.

Erman, J. E. (1974) *Biochemistry 13*, 34−39.

Erman, J. E., Vitello, L., Miller, M. A., Shaw, A., Brown, K. A., & Kraut, J. (1993) *Biochemistry 32*, 9798−9806.

Ferrer, J. C., Turano, P., Banci, L., Bertini, I., Morris, I. K., Smith, K. M., Smith, M., & Mauk, A. G. (1994) *Biochemistry 33*, 7819−7829.

Finzel, B. C., Poulos, T. L., & Kraut, J. (1984) *J. Biol. Chem. 259*, 13027−13036.

Fitzgerald, M., Churchill, M. J., McRee, D. E., & Goodin, D. B. (1994) *Biochemistry 33*, 3807−3818.

Gadsby, P. M. A., & Thomson, A. J. (1990) *J. Am. Chem. Soc. 112*, 5003−5011.

Goodin, D. B., Davidson, M. G., Roe, J. A., Mauk, A. G., & Smith, M. (1991) *Biochemistry 30*, 4953−4962.
Iizuka, T., Makino, R., Ishimura, Y., & Yonetani, T. (1985) *J. Biol. Chem. 260*, 1407−1412.
Inubushi, T., & Becker, E. D. (1983) *J. Magn. Reson. 51*, 128−133.
Kaput, J., Goltz, S., & Blobel, G. (1982) *J. Biol. Chem. 257*, 15054−15058.
Kobayashi, N., Nozawa, T., & Hatano, M. (1977) *Biochim. Biophys. Acta 493*, 340−351.
La Mar, G. N., & de Ropp, J. S. (1993) in *Biological Magnetic Resonance* (Berliner, L. J., & Reuben, J., Eds.) Vol. 12, pp 1−78, Plenum Press, New York.
La Mar, G. N., Chatfield, M. J., Peyton, D. H., de Ropp, J. S., Smith, W. S., Krishnamoorthi, K., Satterlee, J. D., & Erman, J. E. (1988) *Biochim. Biophys. Acta 956*, 267−276.
Macura, S., Wüthrich, K. J., & Ernst, R. R. (1982) *J. Magn. Reson. 47*, 351−357.
Marion, D., & Wüthrich, K. J. (1982) *Biochem. Biophys. Res. Commun. 113*, 967−974.
Matsuoka, A., Kobayashi, N., & Shikama, K. (1992) *Eur. J. Biochem. 210*, 337−341.
McLachlan, S. J., La Mar, G. N., & Lee, K.-B. (1988) *Biochim. Biophys. Acta 957*, 430−445.
Miller, V. P., DePillis, G. D., Ferrer, J. C., Mauk, A. G., & Ortiz de Montellano, P. R. (1992) *J. Biol. Chem. 267*, 8936−8942.
Nozawa, T., Kobayashi, N., & Hatano, M. (1976) *Biochim. Biophys. Acta 427*, 652−662.
Rajarathnam, K., La Mar, G. N., Chiu, M. L., Sligar, S. G., Singh, J. P., & Smith, K. M. (1991) *J. Am. Chem. Soc. 113*, 7886−7892.
Rawlings, J., Stephens, P. J., Nafie, L. A., & Kamen, M. D. (1977) *Biochemistry 16*, 1725−1729.
Satterlee, J. D., & Erman, J. E. (1991) *Biochemistry 27*, 4398−4405.
Satterlee, J. D., Erman, J. E., Mauro, M. J., & Kraut, J. (1990) *Biochemistry 29*, 8797−8804.
Smulevich, G., Mauro, J. M., Fishel, L. A., English, A. M., Kraut, J., & Spiro, T. G. (1988) *Biochemistry 27*, 5477−5485.
Smulevich, G., Miller, M. A., Kraut, J., & Spiro, T. G. (1991) *Biochemistry 30*, 9546−9558.
Stephens, P. J., Sutherland, J. C., Cheng, J. C., & Eaton, W. A. (1976) in *Excited States of Biological Molecular Processes*. (Birks, J. B., Ed.) pp 434−442, Wiley, Chichester.
Unger, S. W., Lecomte, J. T. J., & La Mar, G. N. (1985) *J. Magn. Reson. 64*, 521−526.
Vickery, L., Nozawa, T., & Sauer, K. (1976a) *J. Am. Chem. Soc. 98*, 343−350.
Vickery, L., Nozawa, T., & Sauer, K. (1976b) *J. Am. Chem. Soc. 98*, 351−357.
Vitello, L. B., Huang, M., & Erman, J. E. (1990) *Biochemistry 29*, 4283−4288.
Vitello, L. B., Erman, J. E., Miller, M. A., Mauro, J. M., & Kraut, J. (1992) *Biochemistry 31*, 11524−11535.
Vitello, L. B., Erman, J. E., Miller, M. A., Wang, J., & Kraut, J. (1993) *Biochemistry 32*, 9807−9818.
Vold, R. L., Waugh, J. S., Klein, M. P., & Phelps, D. E. (1968) *J. Chem. Phys. 48*, 3831−3832.
Yamamoto, Y. (1993) *Biochem. Biophys. Res. Commun. 196*, 348−354.
Yonetani, T., & Anni, H. (1987) *J. Biol. Chem. 262*, 9547−9554.

BI950686L